Journal of Applied Polymer Science

# Preparation of PolyHIPE/Clay Composites by Using a Reactive Intercalant

**Funda Çira, Elif Berber, Sinan Şen, E. Hilal Mert**
Department of Polymer Engineering, Yalova University, Yalova, 77100, Turkey
Correspondence to: E. H. Mert (E-mail: hmert@yalova.edu.tr)

**ABSTRACT:** Porous polymer composites have been synthesized by polymerizing the continuous phase of styrene/divinylbenzene high internal phase emulsions in the presence of organophilic montmorillonite clay having a novel oil-based intercalant which is a reactive methacryl derivative of quaternized methyl oleate. The morphological features, thermal stability and mechanical properties, namely compression modulus and crush strength of the resulting composites have been investigated as a function of degree of nanoclay loading. All the composites reinforced with the clay were found to have improved thermal and mechanical properties as well as desired porous and interconnected structural morphology, as compared with the bare polyHIPE matrix. © 2014 Wiley Periodicals, Inc. J. Appl. Polym. Sci. **2015**, *132*, 41333.

**KEYWORDS:** composites; morphology; porous materials; thermosets

Received 14 April 2014; accepted 27 July 2014
**DOI: 10.1002/app.41333**

## INTRODUCTION

Porous monoliths have been attracting much attention in the fields of engineering, adsorption, catalysis, biological, and medical applications such as tissue engineering, drug delivery, enzyme immobilization, and protein purification.[1–11] Porous monoliths can be prepared by different approaches.[2,12] Among them, emulsion templating based on the polymerization of continuous phase of a high internal phase emulsion (HIPE), is a versatile one for the preparation of cellular polymers with a well-defined porosity.[10–12] HIPEs are concentrated emulsion systems consisting of a high ratio of internal or dispersed phase. The volume fraction of the internal phase (Ø) of a HIPE is usually greater than 0.74. In case of, either one or both phases of a HIPE contain monomers, they can be crosslinked to produce polymers, so-called polyHIPEs.[13,14] PolyHIPEs are low-density materials which usually have density lower than 0.1 g $cm^{-3}$. In addition, surface areas of polyHIPEs usually varied between 3 and 20 $m^2$ $g^{-1}$ along with the possibility of increasing this value by modifying the preparation conditions.[15]

Since the Unilever researchers, Barby and Haq[13] prepared the first patented polyHIPE from styrene (St) and divinylbenzene (DVB), the main subject was focused on varying the continuous phase in order to prepare functional materials and controlling the morphology. In this respect, many studies have been made by researchers to modify the polyHIPE surfaces by using the mixture of functional monomers and crosslinker co-monomers such as 4-vinylbenzyl chloride (VBC),[16–18] 2-hydroxyethyl methacrylate (HEMA),[19] glycidyl methacrylate (GMA).[20–22] Recently extensive research focused on the preparation of polyHIPE composites and nanocomposites in order to improve the chemical, thermal and mechanical properties and as well as to find out the major industrial applications. PolyHIPE composites were first developed and published by Menner et al.[23] by introducing 10 to 30 wt % $SiO_2$ particles (relative to monomers) into the organic phase of concentrated emulsions consisting of polyethylene glycol dimethacrylate (PEGDMA), St and methacryloxypropyltrimethoxysilane (MPS). Such polyHIPEs were characterized by significantly high Young's modulus and crush strength in comparison to the polyHIPEs that were prepared without adding $SiO_2$ particles. Afterwards, many studies have been done to obtain polyHIPEs with high mechanical performance by adding silylated silica particles into the continuous phase of HIPEs and medium internal phase emulsions (MIPEs),[24] carbon nanotubes,[25] $TiO_2$ nanoparticles,[25,26] titania nanorods,[25] and organoclays[27–29] into the continuous phase of emulsion templates.

Montmorillonite is a layered silicate having a wide range application in preparation of composite materials. However, the hydrophilic nature of montmorillonite is a big problem for its use to obtain homogeneous dispersions with hydrophobic organic matrixes. This disadvantage can be overcome by a simple surface modification process via organic ammonium cations through an ion exchange reaction. It is known that the increase in d-spacing or the degree of expansion of the clay layers, depends on the cations located in the interlayer region. If the

interlayer cations are mono-valent and strongly hydrated ($Na^+$, $Li^+$), the inter-platelet repulsion is stronger and the degree of platelet separation is larger.[30–32]

The first significant result for polyHIPEs with improved thermomechanical properties by the use of an organophilic montmorillonite nanoclay was published by Deleuze et al.[33] They prepared polyHIPE nanocomposites by adding organophilic montmorillonite nanoclay in 1–20 wt % into the St/DVB concentrated emulsions. In the end, they achieved to obtain polyHIPEs with remarkably high Young's modulus compared to the bare polymer matrix.

Preparation of polyHIPE composites by introducing hybrid organic-inorganic porous clay heterostructures (HPCHs) was carried out by Nithitanakul et al.[27] They synthesized polyDVB polyHIPE materials by introducing 1 to 10 wt % (relative to monomer composition) of pre-synthesized organo-modified bentonite (HPCH) into the continuous phase of HIPEs and investigated their morphological, thermal and mechanical properties. However the results of that study indicate that the mechanical properties did not change proportionally with the amount of nanoclay loading. The resultant polyHIPE composites were found to have compressive stress and Young's modulus changing randomly from 0.0771 to 0.1424 MPa, and from 0.8840 MPa to 2.0979 MPa, respectively.

More recently, Moghbelli and Shahabi[29] prepared poly(2-ethylhexyl acrylate/styrene/divinyl benzene) (poly(EHA/St/DVB)) polyHIPEs by adding 1 to 5 wt % (based on total organic phase) of organically modified sodium montmorillonite organoclays into the monomer phase before emulsification. They discussed the mechanical strengths of the resulting polyHIPEs as a function of the organoclay amount. However, these materials also did not exhibit desired mechanical properties such that the Young's moduli and the crush strengths of the resulting composites were found to have an irregular change with increasing organoclay amount.

In this study, we used a similar approach with the abovementioned studies for the preparation of St/DVB polyHIPE/clay composites. Factors affecting the surface area, cell structure and pore size of the St/DVB polyHIPEs have been explored with various studies. It is well-known from the literature that these polyHIPEs are low-density materials which possess an open cellular structure consisting of cavities connected to each other. Due to the simplicity of the HIPE preparation and providing the emulsion stability, St/DVB polyHIPEs are known to be suitable materials for flow-through processes. It is also known from the previous studies that electrophilic aromatic substitution reactions, namely sulfonation, nitration and bromination can be used for the modification of these polyHIPEs for variety of applications.[34]

Herein, we aimed to investigate the effect of introducing a surface modified organoclay onto the morphological, mechanical and thermal properties of the St/DVB polyHIPEs. Since the major application features are determined by the abovementioned properties, it is important to tailor them by controlling the emulsion composition and preparation conditions. With this respect, we used an oil-based intercalant, which is a reactive

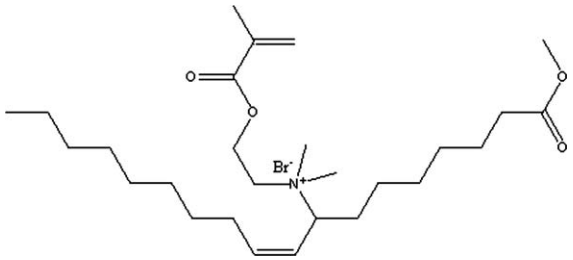


**Figure 1.** Chemical structure of the quaternized methyl oleate (QMO).

methacryl derivative of quaternized methyl oleate (QMQ), in order to render the MMT organophilic character. The QMO is expected to intercalate between the clay layers via ionic exchange reaction between the cations in the interlayer region of the clay and quaternary ammonium cation of the intercalant. Thus, this intercalation can cause a higher expansion of clay galleries with the help of longer moiety of the QMO which acts as an effective spacer. So, this can lead to well distribution of layered silicates in the matrix system as the target of many composite studies. Moreover, the use of this reactive intercalant for the modification of MMT clay is thought to be more effective in preparation of poly(St/DVB/OrgMMT) composites since the organic and reactive modifier group in the intercalant is expected to participate in polymerization/cross-linking reactions via their reactive double bonds which may lead to enhanced thermomechanical properties. The effect of organoclay content on the thermal, mechanical and morphological properties of the resultant polyHIPE composites are discussed in detail.

## EXPERIMENTAL

### Materials

Styrene (St; ≥99%, contains 10–15 ppm 4-tert-butylcatechol as inhibitor), divinylbenzene (DVB; 80% contains divinylbenzene, ethylstyrene, 4-butylpyrocatechol) and sorbitan monooleate (Span 80) were obtained from Aldrich (Steinheim, Germany) as analytical grade and used as received. 2,2'-Azoisobutyronitrile (AIBN) was obtained from Merck (Darmstadt, Germany) and dried in vacuum at room temperature. The clay, sodium montmorillonite (NaMMT) was kindly donated by Süd Chemie, (Moosburg, Germany) (Nanofil 1080; cationic ($Na^+$) exchange capacity of 100 meq/100 g). N,N-(dimethylamino) ethyl methacrylate (DMAEM) and methyl iodide were purchased from Aldrich (Steinheim, Germany) and used as received. Synthesis of methacryl-functionalized quaternary ammonium salt of the allylic brominated methyl oleate intercalant (QMO) (Figure 1) was carried out in a similar manner to that reported previously.[35] It was synthesized from olive oil triglyceride by following three transformations which were transesterification, allylic bromination and quaternization reaction with DMAEM, respectively.

### Methods

**Modification of NaMMT Clay.** NaMMT (2 g) was dispersed in a 300 mL solvent mixture of tetrahydrofuran (THF) and deionized water in which the volume ratio of THF/water solvent mixture is 1/3. A separate solution of 2 g quaternized methyl oleate (QMO) (Figure 1) in the same amount of solvent mixture and

composition was slowly added to the clay solution and mixed vigorously, while keeping the temperature of the solution at 50°C for 4 h. The organically modified MMT was recovered by filtering the solution, followed by repeated washings of the filter cake with THF-deionized water mixture to remove any excess ions. The final product (OrgMMT) was dried at 50°C in a vacuum oven for 48 h.

**Preparation of PolyHIPE Composites.** In a typical experiment, HIPE consists of 90 vol % internal phase (water) and 10 vol % continuous phase. St (4.0905 g) and DVB (0.4570 g) were used as monomer and cross-linker, respectively. Continuous phase of HIPEs were prepared by dissolving surfactant Span 80 (1.4850 g: 30 vol % in regard to monomer composition) and initiator AIBN (0.0910 g: 2 mol % in regard to monomer composition) in the monomer mixture. Organophilic, reactive and pre-expanded nanoclay particles (OrgMMT) (1–3 wt % in regard to monomer composition) were added into the continuous phase. Water was added drop-wise to the continuous phase under constant stirring at 300 rpm. The emulsion was stirred for another 10 min after the addition of water. After a cream-like emulsion was obtained, the emulsion was transferred to the polyethylene mold and cured for 24 h at 70°C. The resulting polymer foam was purified by soxhlet extraction (ethanol, for 24 h), dried under vacuum at 60°C and weighed. In each case the weight of the residue was negligible.

### Characterization

Physicochemical and Morphological Characterization. X-ray diffraction (XRD) measurements of NaMMT and OrgMMT clays as well as composites were conducted on a Rigaku D/Max-Ultimate diffractometer (Rigaku, Tokyo, Japan) with $CuK_{\alpha}$ radiation ($\lambda = 1.54$ Å), operating at 40 kV and 40 mA and a scanning rate of 0.2 deg/min.

Morphological features of polyHIPEs were investigated by scanning electron microscopy (SEM) analysis, using ESEM-FEG and EDAX Philips XL-30 microscope (Philips, Eindhoven, The Netherlands). Prior to SEM analysis polyHIPE samples were cut into small pieces of 1 mm x 1mm, mounted on a copper stub and a thin layer of gold was sprayed on the samples. SEM micrographs were used for the determination of average cell diameters and interconnecting pore diameters. For this purpose, over 50 measurements were taken from each SEM image and the average value was corrected with a correction factor ($2/3^{1/2}$) to account for irregular cutting of the samples.

Specific surface areas, pore sizes and pore volumes were measured with Quantachrome's Autosorb-6B Surface Area and Pore Size Analyzer (Quantachrome GmbH & Co. KG, Germany) by using the Brunauer–Emmet–Teller (BET) molecular adsorption method. Prior to analysis, samples were degassed for 24 h at 70°C. The densities of the resulting foams were measured by using a Sartorius ED224S Analytical Balance (Sartorius AG, Germany) equipped with a density determination kit.

**Thermal Analysis**. Thermogravimetric analyses (TGA) of the polyHIPEs were performed on a Seiko TG/DTA 6300 thermal analysis system instrument (Seiko Instruments, Tokyo, Japan) under nitrogen flow with a heating rate of 10 °C/min. The differential scanning calorimeter (DSC) measurements were performed on a Seiko DSC 7020 calorimeter (Seiko Instruments) to measure glass transition temperatures of the samples by using instrument at a heating rate of 10°C/min. During DSC measurements two heating and one cooling curves were recorded for each sample in a temperature range from 10 to 300°C and the heat flow was measured. However we did not observe any thermal transition most probably due to the highly cross-linked structure. For this reason DSC profiles were not introduced in the present paper.

Mechanical Characterization. The mechanical strengths of the polyHIPE samples were measured by performing uniaxial compression experiment with a Zwick/Roell Z020 Universal Testing Machine (Zwick GmbH & Co.KG, Germany) equipped with a 20 kN load cell. All the mechanical measurements were performed on the samples which are cut into cylindrical samples of about 15 mm in diameter and 10 mm in height at room temperature and at a compression rate of 4 mm/min. The measurements were conducted until a displacement of 80% of the examined sample was reached. The crush strength as the maximum strength as well as compression modulus were obtained from the original output of the instrument.

## RESULTS AND DISCUSSION

### Modification of NaMMT Clay

Modification of the MMT clay was followed by XRD and TGA analyses. XRD analysis gave the values of the interlayer spacing or d-spacing of the NaMMT and OrgMMT which were obtained from the peak position of the $d_{001}$ reflection in the diffraction patterns (Figure 2). The XRD data for the clays are given in Table I. A $2\theta$ angle of 7.28° and basal spacing of 12.13 Å was found for NaMMT clay. It can be seen from Table I and Figure 2 that the interlayer spacing values of the OrgMMT was found to be 25.81 Å with a decrease in its diffraction angle (3.41°). Thus, a decrease in the diffraction angle and increase in interlayer distance indicates that intercalation of the intercalant into MMT clay layers through the ion-exchange reaction was successful, resulting in organophilic clay.

The existence of the intercalant in the MMT structure was also confirmed by TGA. Figure 3 shows the TGA thermograms of NaMMT and OrgMMT. It is clear from the figure that OrgMMT shows a lower decomposition onset temperature as well as higher degradation dependent weight loss compared to pure NaMMT. Pure MMT has only 7.2% total weight loss indicating water removal. After the intercalation, this amount reaches almost 26.4% at higher temperatures, resulting from the degradation of intercalated and edge/surface attached methyl oleate (Figure 3(a)]. As it can be seen from the first derivative curves of the weight loss [Figure 3(b)] that NaMMT was found to have two distinctive weight loss at 60°C and 600°C most probably due to removal of moisture and bound water present in the clay galleries, respectively.[36,37] On the other hand, TGA traces of the OrgMMT were completely different. OrgMMT showed maximum weight loss at temperatures, 270°C, 375°C and 430°C, with much higher weight loss compared to NaMMT clay. This result can be accepted as an indication of the successful modification of the MMT clay.

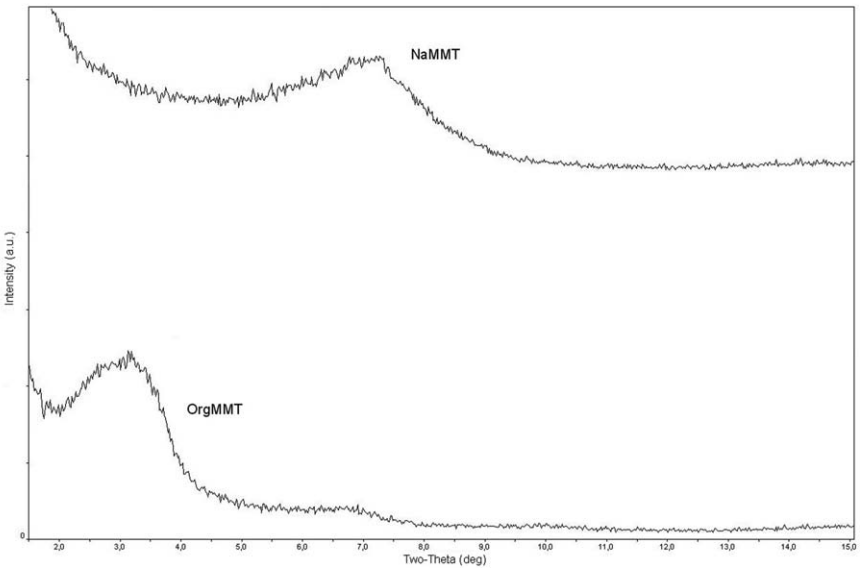


**Figure 2.** XRD patterns of NaMMT and OrgMMT.

### Structural Characterization of PolyHIPE Composites

PolyHIPE composites were obtained by the cross-linking of the emulsions prepared by dispersing the OrgMMT particles in 1–3 wt % loading in the continuous phase of the St/DVB emulsions. The degree of dispersion of organophilic clay in polyHIPE matrix was determined by XRD analyses. Figure 4 shows X-ray diffractograms of the resulting composites (P2, P3, and P4). As it can be seen from the figure, there is no noticeable MMT clay peak ($d_{001}$ reflection) appearing in their diffraction patterns as an indication of delaminated composite structure.[30] This result may be attributed to the good swelling of OrgMMT clay having an oil-based intercalant in St/DVB monomer mixture and homogeneous dispersion of the clay layers in the matrix. Both existence of certain amount of clay intercalation via peak shift from 12.13 Å to 25.81 Å and TGA confirmation (Figure 3) show the succesful organophilization of MMT layers from interlayer galleries and edges/surfaces of the clay. During polyHIPE composite formation, possible pulling of silica layers with styrene monomer through participation of edge-surface attached QMO in polymerization may contribute to a further delamination of silicate layers.[30]

### Morphological Properties

It is well known from the literature that in case of polymer composite systems, chemical composition, concentration, size and wettability of the nanoparticles directly affect the emulsion stability and the morphology of the final polymer product.[38,39] Depending on the fact that emulsions are thermodynamically unstable, incorporation of nanoparticles into the continuous phase of an emulsion may lead to particle coagulation, which is the major factor influencing the stability of the emulsions by causing emulsion disintegration or phase inversion with heating. Thus, surface modification or structural modification of nanoparticles is essential for the control of the properties of the final product by controlling the emulsification parameters. In this work, we observed that the organophilic nanoclay (OrgMMT) particles did not yield a significant effect on the emulsion stability and the emulsions preserved their stabilities at room temperature for a long time.

The effect of the degree of nanoclay loading on morphological properties of the polyHIPE composites was investigated by SEM analyses and SEM images are presented in Figure 5. The distinctive property of polyHIPEs is their special morphology consisting of cavities connected by small channels. In some cases, the size of the channels and cavities are so close thus fibrilar mesh morphology formed instead of the familiar pore structure.[40] According to the SEM images given in Figure 5, the bare polyHIPE sample (P1) and all the polyHIPE composites exhibited a porous structure with an open cellular architecture. However, the resulting materials exhibited fibrilar mesh morphology rather than the usual polyHIPE morphology. The resulting composites seem to compose of pores surrounded by polymer layers. The pore size analyses of the given SEM micrographs exhibited that the diameter of the pores are about 6 μm for the composites (Table II). This result indicates that addition of OrgMMT particles caused a slight decrease of pore diameter compared with the bare polyHIPE sample. Accordingly, P3 and P4 composites were found to have almost three times more surface area than bare polyHIPE matrix which was obtained by BET adsorption measurements (Table II). This remarkable increase in surface area can be explained by the formation of fibrilar mesh morphology.

### Thermal Properties

The thermal stability of the pure polyHIPE matrix and the composites were studied by thermogravimetric analysis (TGA) and

**Table I.** XRD Data for Clays

| Material | $D_{001}$ of clay (Å)[a] |
|---|---|
| NaMMT | 12.13 (7.28°) |
| OrgMMT-1 | 25.81 (3.41°) |

[a] Two-Theta angles are given in parentheses.

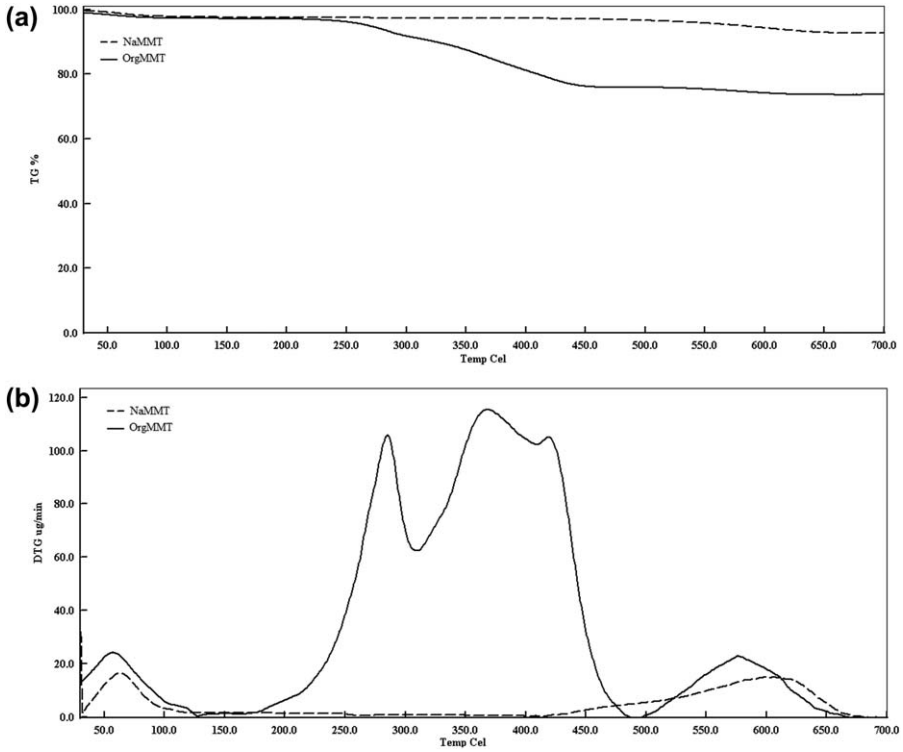


**Figure 3.** TGA and DTG thermograms of NaMMT and OrgMMT.

the results are presented in Table III and Figure 6. The onset and the mid-point degradation temperatures, $T_{d10}$ and $T_{d50}$, represents the temperatures at which 10 wt % and 50 wt % degradation occurs, respectively. As it can be seen from Table III these temperatures increased prominently for polyHIPE composites with the increase of nanoclay amount compared with the pure polyHIPE matrix. It is clear from the table that compared to the pure polyHIPE matrix, the highest increments in the onset and the mid-point degradation temperatures were observed for the composite P3 which was prepared via adding OrgMMT in 2 wt % loading. It was calculated from the TGA data given in Table III that $T_{d10}$ and $T_{d50}$ were increased by almost 72°C and 50°C, respectively, for P3.

Higher thermal stability in P2, P3, and P4 composites might be attributed to extensive interaction between the OrgMMT clay and the polymer matrix resulted from the larger surface area of the clay arised from its oil-based intercalant and the participation of organoclay into polymerization/crosslinking reaction through its methacryl and allylic groups.[41–43] This maximized interaction may lead to restricted molecular mobility of the polymer chains resulting in inhibition of the diffusion of the decomposed product in the polymer matrix.[44] Moreover, the DTGA thermograms of the samples (Figure 6) show that the temperature at which the maximum weight loss occur was also increased almost 49°C for the resultant composites. Although composite P2 seem to have relatively lower degradation rate for maximum weight loss, it was found to lose 10% of its weight loss at a much earlier temperatures compared to composite polyHIPEs, P3 and P4 (Table III). Therefore, it can be safely stated that P3 composite with the highest onset and mid-point degradation temperatures has the highest thermal stability relative to the bare polyHIPE matrix and other composites. The char yield was also found to be increased as expected with the degree of OrgMMT loading.

### Mechanical Properties

Mechanical properties of the polyHIPE composites were investigated in terms of compression strength. The compression stress-strain data of the composites are shown in Figure 7 and Table IV. The compression moduli of the all polyHIPE composites were found to be higher than the bare polyHIPE matrix and increase when clay loading increases. The maximum modulus was obtained for P4 composite sample having the highest clay amount, leading to the highest resistance to deformation which is in good agreement with its lowest compressibility (Figure 7). The lowest crush strength of P2, on the other hand, might be

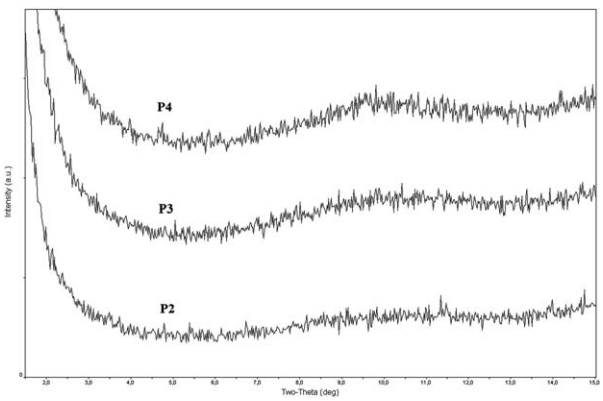


**Figure 4.** XRD patterns of the resulting composites.

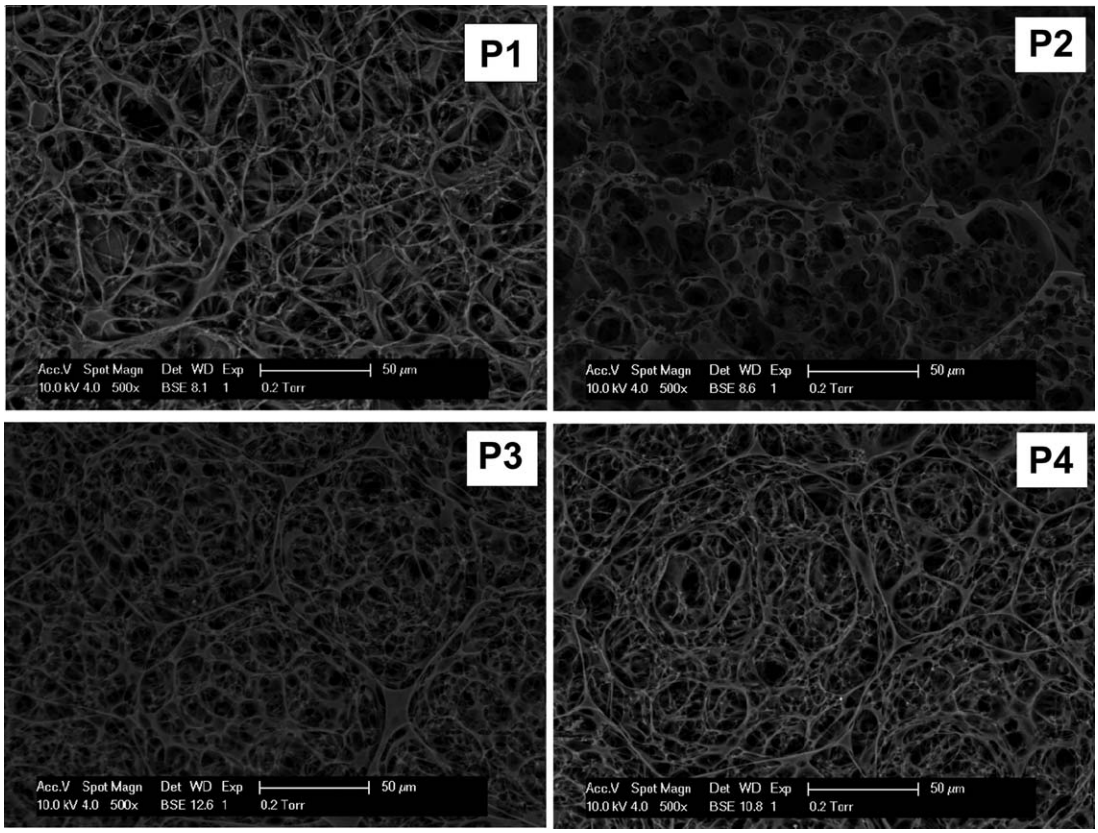


**Figure 5.** SEM micrographs of the resulting polyHIPEs.

due to its more viscous character in presence of oil-based intercalant at 1% clay loading. The effect of reactive double bonds in the intercalant on the mechanical strength seems to be effective above 1% clay loading.

P3 exhibited the highest the crush strength. This result may be ascribed to the incorporation of well-dispersed organophilic nano-platelets having reactive and oil-based intercalant into crosslinked network in 2 wt % OrgMMT loading as optimum clay amount. The highest mechanical strength of P3 sample may be attributed to the formation of sub-networks having extended crosslinking chains resulted from the abovementioned contribution of the clay to polymerization/crosslinking reaction through its metharyl and allylic groups.[41–43] This additional chemical cross-links may also help in sharing the applied compressive forces effectively. This "effective" participation of clay particles into the crosslinking reaction may also lead to formation of a stretchable microcomplex structure due to the existence of higher amount of ionic interaction of negatively charged nano-sized clay surface and positively charged quaternary ammonium groups connected to network matrix throughout the covalent bonds. These sites may act as a kind of reversible physical crosslinking causing a more viscous network structure,[45,46] leading to high compressibility observed for the composite.

The lower crush strength of P4 may be attributed to the existence of relatively more attractive forces between the clay layers at high loading[47] leading to less reversible ionic interaction sites for the polymer matrix and its more rigid structure inhibiting deformation at the highest clay loading.

## CONCLUSIONS

Poly(styrene/divinylbenzene/organophilic montmorillonite) (poly(St/DVB/OrgMMT)) composites were successfully prepared by polymerization of the continuous phase of HIPEs in the presence of an organophilic montmorillonite (MMT) clay.

**Table II.** Nanoclay Type and Amount and Morphological Properties of PolyHIPEs

| Sample ID | Nanoclay loading (wt %) | Surface area ($m^2\ g^{-1}$) | Pore size (μm) | Pore volume ($mL\ g^{-1}$) | Density ($g\ mL^{-1}$) |
|---|---|---|---|---|---|
| P1 | - | 13.65 ± 2.05 | 8.61 ± 0.65 | 0.081 ± 0.002 | 0.1198 |
| P2 | 1 | 18.40 ± 1.62 | 6.92 ± 0.38 | 0.036 ± 0.013 | 0.2955 |
| P3 | 2 | 31.60 ± 3.89 | 6.42 ± 0.39 | 0.135 ± 0.049 | 0.2486 |
| P4 | 3 | 40.93 ± 4.32 | 6.37 ± 0.46 | 0.115 ± 0.040 | 0.2681 |

**Table III.** Thermal Stability of PolyHIPEs

| Sample ID | $T_{d10}$ (°C) | $T_{d50}$ (°C) | Maximum rate of weight loss (% $min^{-1}$ at °C) | Char (wt %) |
|---|---|---|---|---|
| P1 | 317.9 | 373.8 | 10.09 at 375.2 | 0.18 |
| P2 | 375.5 | 418.1 | 8.63 at 378.1 | 0.66 |
| P3 | 389.9 | 423.3 | 12.8 at 411.5 | 3.22 |
| P4 | 383.5 | 421.6 | 18.1 at 424.0 | 5.96 |

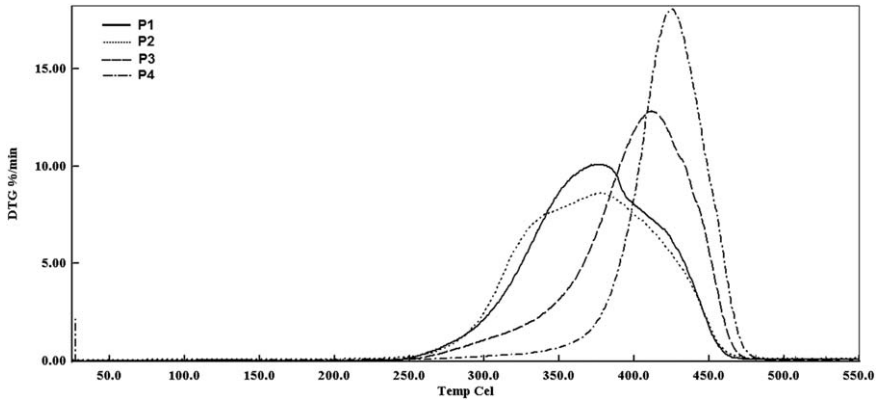


**Figure 6.** Comparative DTGA thermograms of the resulting polyHIPEs.

Organically and functionally modified OrgMMT clay was used as reinforcer in three different loading degrees (1, 2, and 3 wt %). The organophilic modification of NaMMT clay was carried out with quaternized methyl oleate (QMO) which is a renewable intercalant having a reactive methacryl group. The contribution of OrgMMT presence in the polymer matrix on the properties of poly(St/DVB/OrgMMT) composites were discussed in terms of morphological, thermal and mechanical properties. The success in intercalation of the intercalant into MMT clay layers through the ion-exchange reaction and dispersion of clays in polymer matrix were confirmed via XRD and TGA. The X-ray diffractograms of the polyHIPE composites did not show any noticeable MMT clay peak ($d_{001}$ reflection) appearing in their diffraction patterns most probably due to the homogeneous dispersion of the clays, which does not present any more ordering, or a too large spacing between the layers. The resulting composites were found to have higher thermal stability and better mechanical properties as compared to the bare polymer matrix. This is probably due to the polymerization/crosslinking reaction occurring in between the highly expanded and homogeneously dispersed silicate layers and from the edge/surface of the modified clay through the intercalated and edge/surface attached reactive intercalant. Furthermore, SEM images of the polyHIPE composites indicated highly porous and interconnected morphology. The pore size analyses showed that the pore diameters were decreased slightly by the addition of OrgMMT particles in 3 wt %, while the BET surface areas increased remarkably. As a result it can be safely concluded that polyHIPE composites with different degrees of thermal stability and mechanical strength can be prepared by using a matrix compatible, functionally and organically modified clay in 1–3 wt % clay loadings.

Further research will be focused on the modification of resulting St/DVB polyHIPE composites by electrophilic substitution

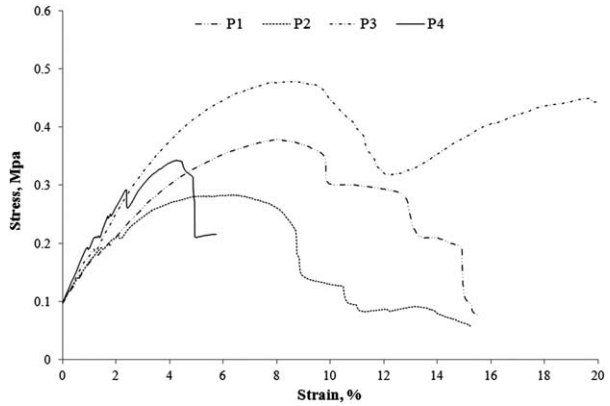


**Figure 7.** Comparative stress–strain curves of the resulting polyHIPEs.

**Table IV.** Mechanical Properties of PolyHIPEs

| Sample ID | Compressive modulus (MPa) | Crush strength (MPa) |
|---|---|---|
| P1 | 7.17 ± 0.15 | 0.38 ± 0.021 |
| P2 | 7.88 ± 0.28 | 0.28 ± 0.032 |
| P3 | 8.84 ± 0.21 | 0.48 ± 0.023 |
| P4 | 12.16 ± 0.55 | 0.34 ± 0.043 |

reactions and will be followed by investigating the effectiveness of these materials as adsorbents for various organic pollutants.

## REFERENCES


1. Nischang, I. *J. Chromatogr. A.* **2013**, *1287*, 39.
2. Vázquez, M.; Paull, B. *Anal. Chim. Acta.* **2010**, *668*, 100.
3. Svec, F. *J. Chromatogr. A.* **2010**, *1217*, 902.
4. Huang, X.; Dasgupta, P. K. *Anal. Chim. Acta.* **2011**, *689*, 155.
5. Nischang, I.; Teasdale, I.; Brüggemann, O. *J. Chromatogr. A.* **2010**, *1217*, 7514.
6. He, H.; Li, W.; Zhong, M.; Konkolewicz, D.; Wu, D.; Yaccato, K.; Rappold, T.; Sugar, G.; David, N. E.; Matyjaszewski, K. *Energy Environ. Sci.* **2013**, *6*, 488.
7. Xu, F.; Zhang, N.; Long, Y.; Si, Y.; Liu, Y.; Mi, X.; Wang, X.; Xing, F.; You, X.; Gao, J. *J. Hazard. Mater.* **2011**, *188*, 148.
8. El-Feky, H. H.; Àngels, Cano-Òdena.; Gumí, T. *J. Membr. Sci.* **2013**, *439*, 96.
9. Arrua, R. D.; Moya, C.; Bernardi, E.; Zarzur, J.; Strumia, M.; Igarzabal, C. I. A. *Eur. Polym. J.* **2010**, *46*, 663.
10. Kimmins, S. D.; Cameron, N. R. *Adv. Funct. Mater.* **2011**, *21*, 211.
11. Silverstein, M. S.; Cameron, N. R.; Hillmyer, M. A. Porous Polymers; Hoboken, New Jersey, **2011**.
12. Svec, F. *J. Chromatogr. A.* **2010**, *1217*, 902.
13. Barby, D.; Haq Z. U.S. Pat. 4522953, **1985**.
14. Cameron, N. R. *Polymer* **2005**, *46*, 1439.
15. Cameron, N. R.; Sherrington, D. C. *Adv. Polym. Sci.* **1996**, *126*, 163.
16. Štefanec, D.; Krajnc, P. *React. Func. Polym.* **2005**, *65*, 37.
17. Jerábek, K.; Pulko, I.; Soukupova, K.; Štefanec, D.; Krajnc, P. *Macromolecules* **2008**, *41*, 35.
18. Krajnc, P.; Leber, N.; Brown, J. F.; Cameron, N. R. *React. Func. Polym.* **2006**, *66*, 81.
19. Cameron, N. R.; Sherrington, D. C. *J. Mater. Chem.* **1997**, *7*, 2209.
20. Barbetta, A.; Dentini, M.; Leandri, L.; Ferraris, G.; Coletta, A.; Bernabei, M. *React. Func. Polym.* **2009**, *69*, 724.
21. Krajnc, P.; Leber, N.; Stefanec, D.; Kontrec, S.; Podgornik, A. *J. Chrom. A* **2005**, *1065*, 69.
22. Mert, E. H.; Kaya, M. A.; Yıldırım, H. *Des. Monomers. Polym.* **2012**, *15*, 113.
23. Menner, A.; Haibach, K.; Powell, R.; Bismarck, A. *Polymer* **2006**, *47*, 7628.
24. Wu, R.; Menner, A.; Bismarck, A. *J. Polym. Sci., Part A: Polym. Chem.* **2010**, *48*, 1979.
25. Menner, A.; Salgueiro, M.; Shaffer, M. S. P.; Bismarck, A. *J. Polym. Sci., Part A: Polym. Chem.* **2008**, *46*, 5708.
26. Ikem, V. O.; Menner, A.; Bismarck, A. *Langmuir* **2010**, *26*, 8836.
27. Pakeyangkoon, P.; Magaraphan, R.; Malakul, P.; Nithitanakul, M. *J. Appl. Polym. Sci.* **2009**, *114*, 3041.
28. Abbasian, Z.; Moghbeli, M. R. *J. Appl. Polym. Sci.* **2011**, *119*, 3728.
29. Moghbeli, M. R.; Shahabi, M. *Iran Polym. J.* **2011**, *20*, 343.
30. Alexandre, M.; Dubois, P. *Mater. Sci. Eng. R: Reports* **2000**, *28*, 1.
31. Luckham, P. F.; Rossi, S. *Adv. Colloid Interface Sci.* **1999**, *82*, 43.
32. Hunter, R.J. Foundations of Colloid Science; Oxford Univ. Press: New York, **1986**; Vol. *1*, p 673.
33. Lépine, O.; Birot, M.; Deluze, H. *J. Polym. Sci., A: Polym. Chem.* **2007**, *45*, 4193.
34. Cameron, N. R.; Sherrington, D. C.; Andob, I.; Kurosu, H. *J. Mater. Chem.* **1996**, *6*, 719.
35. Albayrak, O.; Sen, S.; Caylı, G.; Ortac, B. *J. Appl. Polym. Sci.* **2013**, *130*, 2031.
36. Pansu, M.; Gautheyrou, J.; Handbook of Soil Analyses. Mineralogical, Organic and Inorganic Methods; Springer: Berlin, Heidelberg, New York; 2006; Chapter 1, p 9.
37. Song, K.; Sandi, G. *Clays Clay Miner.* **2001**, *49*, 119.
38. Vílchez, A.; Rodríguez-Abreu, C.; Esquena, J.; Menner, A.; Bismarck, A. *Langmuir* **2011**, *27*, 13342.
39. Mert, E. H.; Yildirim, H.; Üzümcü, A. T.; Kavas, H. *React. Funct. Polym.* **2013**, *73*, 175.
40. Pulko, I.; Krajnc, P. *Macromol. Rapid Common.* **2012**, *33*, 1731.
41. Meyer, V. E. *J. Polym. Sci. Part A: Polym. Chem.* **1966**, *4*, 2819.
42. Paris, R.; De la Fuente, J. L. *React. Funct. Polym.* **2007**, *67*, 264.
43. Venkatesh, R.; Vergouwen, F.; Klumperman, B. *J. Polym. Sci., Part A: Polym. Chem.* **2004**, *42*, 3271.
44. Leszczynska, A.; Njuguna, J.; Pielichowski, K.; Banerjee, J. R. *Thermochim. Acta.* **2007**, *453*, 75.
45. Haraguchi, K.; Li, H. *J. Macromolecules* **2006**, *39*, 1898.
46. Haraguchi, K.; Farnworth, R.; Ohbayashi, A.; Takehisa, T. *Macromolecules* **2003**, *36*, 5732.
47. Koo, C. M.; Ham, H. T.; Choi, M. H.; Kim, S. O.; Chung, I. *J. Polymer* **2003**, *44*, 681.